Priority Report

Cancer Research

PCAT-1, a Long Noncoding RNA, Regulates BRCA2 and Controls Homologous Recombination in Cancer

John R. Prensner[1,2], Wei Chen[3], Matthew K. Iyer[1], Qi Cao[1,2], Teng Ma[4], Sumin Han[3], Anirban Sahu[1], Rohit Malik[1], Kari Wilder-Romans[3], Nora Navone[9], Christopher J. Logothetis[9], John C. Araujo[9], Louis L. Pisters[9], Ashutosh K. Tewari[10], Christine E. Canman[5], Karen E. Knudsen[12], Naoki Kitabayashi[11], Mark A. Rubin[11], Francesca Demichelis[11,13], Theodore S. Lawrence[3], Arul M. Chinnaiyan[1,2,6,7,8], and Felix Y. Feng[1,3,7]

Abstract

Impairment of double-stranded DNA break (DSB) repair is essential to many cancers. However, although mutations in DSB repair proteins are common in hereditary cancers, mechanisms of impaired DSB repair in sporadic cancers remain incompletely understood. Here, we describe the first role for a long noncoding RNA (lncRNA) in DSB repair in prostate cancer. We identify *PCAT-1*, a prostate cancer outlier lncRNA, which regulates cell response to genotoxic stress. *PCAT-1* expression produces a functional deficiency in homologous recombination through its repression of the *BRCA2* tumor suppressor, which, in turn, imparts a high sensitivity to small-molecule inhibitors of *PARP1*. These effects reflected a posttranscriptional repression of the *BRCA2* 3′UTR by *PCAT-1*. Our observations thus offer a novel mechanism of "BRCAness" in sporadic cancers. *Cancer Res; 74(6); 1651–60. ©2014 AACR.*

Introduction

The uncontrolled accumulation of double-stranded DNA breaks (DSB) represents a putative Achilles heel for cancer cells, because these lesions are toxic and their repair requires religation of disrupted genetic material (1–3). Several mechanisms, such as nonhomologous end joining (NHEJ), microhomology-mediated end joining (MMEJ), and homologous recombination (HR), contribute to DSB repair and are employed variously during the cell cycle depending on whether a specific DSB harbors either large, small, or no stretches (NHEJ, MMEJ, and HR, respectively) of complementary DNA sequences on the two fragments of broken DNA (4). In particular, the lethality of excess DSBs has been exploited for the therapeutic treatment of hereditary breast and ovarian cancers harboring *BRCA1/2* mutations, which leads to defective HR and increased DSBs (5). These cancers exhibit synthetic lethality when treated with small-molecule inhibitors of the *PARP1* DNA repair enzyme, whose inhibition prevents a second method of DNA repair and leads to gross collapse of cellular DNA maintenance (6–8).

Recently, long noncoding RNAs (lncRNA) have emerged as new layer of cell biology (9), contributing to diverse biologic processes. In cancer, aberrant expression of lncRNAs is associated with cancer progression (9, 10), and overexpression of oncogenic lncRNAs can promote tumor cell proliferation and metastasis through transcriptional regulation of target genes (11–13). Recent studies have also identified lncRNAs induced by genotoxic stress as well as involved in the repair of DNA damage (14, 15); however, the role of lncRNAs in the regulation of DSB repair remains unclear.

Here, we report the characterization of *PCAT-1* as a prostate cancer lncRNA implicated in the regulation of DSB repair. We find that *PCAT-1* represses the BRCA2 tumor suppressor gene, leading to downstream impairment of HR. Importantly, *PCAT-1*–expressing cells exhibit a BRCA-like phenotype, resulting in cell sensitization to PARP1 inhibitors. In human prostate cancer tissues, high *PCAT-1* expression predicts for low *BRCA2* expression, supporting our observations in model systems. To our knowledge, this report is the first to demonstrate a role for

Authors' Affiliations: [1]Michigan Center for Translational Pathology; Departments of [2]Pathology, [3]Radiation Oncology, [4]Internal Medicine, [5]Pharmacology, and [6]Urology; [7]Comprehensive Cancer Center; [8]Howard Hughes Medical Institute, University of Michigan Medical School, Ann Arbor, Michigan; [9]Department of Genitourinary Medical Oncology, MD Anderson Cancer Center, Houston, Texas; [10]Department of Urology, Institute of Prostate Cancer and LeFrak Center For Robotic Surgery; [11]Department of Pathology and Laboratory Medicine, Weill Cornell Medical College and New York Presbyterian Hospitals, New York, New York; [12]Departments of Cancer Biology, Urology, and Radiation Oncology, Thomas Jefferson University, Philadelphia, Pennsylvania; and [13]Centre for Integrative Biology, University of Trento, Trento, Italy

Note: Supplementary data for this article are available at Cancer Research Online (http://cancerres.aacrjournals.org/).

J. R. Prensner and W. Chen contributed equally to this work.

A.M. Chinnaiyan and F.Y. Feng share senior authorship.

Corresponding Authors: Felix Y. Feng, Department of Radiation Oncology, University of Michigan Medical Center, 1500 E Medical Center Drive, UHB2C490-SPC5010, Ann Arbor, MI 48109-5010. Phone: 734-936-4302; Fax: 734-763-7371; E-mail: ffeng@med.umich.edu; and Arul M. Chinnaiyan, E-mail: arul@med.umich.edu

doi: 10.1158/0008-5472.CAN-13-3159

lncRNAs in the regulation of DSBs in prostate cancer and suggests a new mechanistic basis for impaired HR in this disease.

Materials and Methods

For full details on methodology, please refer to the Supplementary Information for a complete Materials and Methods section.

Patient samples

For the University of Michigan patient samples, prostate tissues were obtained from the radical prostatectomy series and Rapid Autopsy Program at the University of Michigan tissue core. These programs are part of the University of Michigan Prostate Cancer Specialized Program of Research Excellence (SPORE). All tissue samples were collected with informed consent under an Institutional Review Board (IRB) approved protocol at the University of Michigan [SPORE in Prostate Cancer (Tissue/Serum/Urine) Bank IRB # 1994-0481]. For the Weill Cornell Medical College patient samples, prostate tissues were collected as part of an IRB-approved protocol at Weill Cornell Medical College (New York, NY).

Cell lines

All cell lines were obtained from the American Type Culture Collection (ATCC). Cell lines were maintained using standard media and conditions. Du145-derived cell lines were maintained in Dulbecco's Modified Eagle Medium supplemented with 10% FBS (Invitrogen) and 1% penicillin–streptomycin (Invitrogen) in a 5% CO_2 cell culture incubator. RWPE-derived cell lines were maintained in keratinocyte serum-free (Invitrogen) supplemented with bovine pituitary extract, EGF, and 1% penicillin-streptomycin in a 5% CO_2 cell culture incubator. LNCAP-derived and PC3-derived cell lines were maintained in RPMI-1640 (Invitrogen) supplemented with 10% FBS and 1% penicillin-streptomycin in a 5% CO_2 cell culture incubator.

PC3 cells containing the GFP HR assay construct were generated as described previously (16, 17).

PCAT-1 or control-expressing cell lines were generated by cloning *PCAT-1* or control *LacZ* into the pLenti6 vector (Invitrogen). After confirmation of the insert sequence, lentiviruses were generated at the University of Michigan Vector Core and transfected into RWPE or Du145 cells. Stably transfected cells were selected using blasticidin (Invitrogen).

For LNCAP cells with stable knockdown of *PCAT-1*, cells were seeded at 50%–60% confluency, incubated overnight, and transfected with *PCAT-1* or nontargeting short hairpin RNA (shRNA) lentiviral constructs for 48 hours. GFP^+ cells were drug-selected using 1 μg/mL puromycin. *PCAT-1* shRNAs were custom generated by Systems Biosciences using the following sequences: shRNA 1 GCAGAAACACCAAUGGAUAUU; shRNA 2 AUACAUAAGACCAUGGAAAU.

To ensure cell identity, all cell lines were used for less than 6 months after resuscitation and confirmed by genotyping after resuscitation. DNA samples were diluted to 0.10 ng/μL and ten genotyping loci (D3S1358, D5S818, D7S820, D8S1179, D13S317, D18S51, D21S11, FGA, vWA, and the Amelogenin locus) were analyzed by the University of Michigan DNA Sequencing Core using the Profiler Plus PCR Amplification Kit (Applied Biosystems).

Cell line assays

LNCaP, Du145, PC3, and RWPE cell lines were obtained from the ATCC and maintained in standard conditions. Stable overexpression and knockdown cell lines were generated with lentiviral constructs with blasticidin or puromycin selection as appropriate. RNA isolation and cDNA synthesis were performed according to standard protocols. Quantitative PCR was performed with Power SYBR Green Mastermix on an Applied Biosystems 7900HT Real-Time PCR system. Chemosensitivity assays were performed on 5,000 cells plated per well in 96-well plates and treated with a single dose of olaparib or ABT-888 as indicated for 72 hours. WST assays (Roche) were performed according to the manufacturer's instructions. Immunofluorescence experiments were performed with 1×10^5 cells in 12-well plates according to standard protocols; RAD51 and γ-H2AX staining was performed 6 hours or 24 hours after treatment, respectively.

Luciferase assays

The indicated cell lines were transfected with full-length *BRCA2* luciferase constructs as well as pRL-TK vector as internal control for luciferase activity. After 2 days of incubation, the cells were lysed and luciferase assays conducted using the dual luciferase assay system (Promega). Each experiment was performed in quadruplicate.

Immunoblot analysis

Cells were lysed in radioimmunoprecipitation assay lysis buffer (Sigma) and briefly sonicated for homogenization. Aliquots of each protein extract were boiled in sample buffer, size fractionated by SDS-PAGE at 4°C, and transferred onto polyvinylidene difluoride membrane (GE Healthcare). The membrane was then incubated at room temperature for 1 to 2 hours in blocking buffer [Tris-buffered saline, 0.1% Tween (TBS-T), 5% nonfat dry milk] and incubated at 4°C with the appropriate antibody. Following incubation, the blot was washed 4 times with TBS-T and incubated with horseradish peroxidase-conjugated secondary antibody. The blot was then washed 4 times with TBS-T and twice with TBS and the signals visualized by enhanced chemiluminescence system as described by the manufacturer (GE Healthcare).

The following antibodies were used for immunoblot analysis: BRCA2 (EMD, OP95), BRCA1 (Cell Signaling Technology, #9025S), XRCC1 (Abcam, ab1838), XRCC3 (Abcam, ab97390), XRCC4 (GeneTex, GTX83406), Ku70 (BD Biosciences, #611892), Ku80 (Cell Signaling Technology, #2180S), γ-H2AX (Cell Signaling Technology, #9718) and β-actin (Sigma, A5441).

For immunoblot densitometry, the densitometric scan of the immunoblots was performed using ImageJ. Three replicate experiments were quantified for the final analysis.

Xenograft assays

Xenograft experiments were performed according to University of Michigan-approved protocols and conform to their relevant regulatory standards. Five-week-old male severe combined immunodeficient (SCID) mice (CB.17. SCID) were purchased from Charles River, Inc. (Charles River Laboratory). A total of 1×10^6 Du145-control or Du145-*PCAT-1* stable cells were resuspended in 100 μL of saline with 50% Matrigel (BD Biosciences) and were implanted subcutaneously into the left and right flank regions of the mice. Mice were anesthetized using a cocktail of xylazine (80–120 mg/kg, i.p.) and ketamine (10 mg/kg, i.p.) for chemical restraint before tumor implantation. All tumors were staged for 2 weeks before starting the drug treatment. At the beginning of the third week, mice with tumors (10 tumors/treatment group, average size 150–200 mm^3) were treated with olaparib (100 mg/kg, i.p. twice daily five times/week) or an equal volume of dimethyl sulfoxide (DMSO) control. Growth in tumor volume was recorded weekly by using digital calipers.

I-SceI HR assay

We followed previously described protocols (16). Briefly, PC-3 cells with a single copy of DR-GFP were transfected with empty vector control or *PCAT-1*. *PCAT-1*–transfected cells were infected with adenovirus-encoded I-SceI (adeno-I-SceI) at an MOI of 1,000. Cells were harvested 3 days after infection and subjected to flow cytometry analysis for the GFP^+ cell population.

Statistical analyses

All data are presented as means ± SD or SEM, as indicated. All experimental assays were performed in duplicate or triplicate. Statistical analyses shown in figures represent Fisher exact tests or Student *t* tests, as indicated.

Results

PCAT-1 regulates BRCA2 levels and HR

We previously reported the systematic nomination of lncRNAs associated with prostate cancer, termed Prostate Cancer Associated Transcripts (PCAT ref. 10). Among these, we noted that *PCAT-1* expression was a prostate cancer outlier associated with low levels of *BRCA2*. We therefore hypothesized that *PCAT-1* mediated the repression of *BRCA2*, and thus *PCAT-1* may be implicated in the dysregulation of HR upon genotoxic stress. To pursue this hypothesis, we generated a panel of three *in vitro* cell culture model systems: *PCAT-1* overexpression in Du145 prostate cancer cells (which lack endogenous expression of this lncRNA), *PCAT-1* overexpression in RWPE benign prostate cells (which lack endogenous expression of this lncRNA), and stable knockdown of *PCAT-1* in LNCaP prostate cancer cells (which harbor high endogenous levels of *PCAT-1* expression; Fig. 1A, left).

Western blot analysis of these three isogenic models uniformly revealed strong downregulation of BRCA2 protein levels in RWPE and Du145 prostate cells and upregulation of BRCA2 in LNCaP sh-*PCAT-1* cells (Fig. 1A, right). To ensure that these observations were not restricted to cell line-based studies, we further confirmed an inverse relationship between *PCAT-1* and *BRCA2* in two independent cohorts of human prostate cancer samples. Using 58 prostate cancer tissues and 20 prostate cancer xenografts derived from human specimens, we found that increasing *PCAT-1* expression correlated with decreased *BRCA2* expression (Fig. 1B and Supplementary Fig. S1A). Together, these data suggest that *PCAT-1* expression antagonizes *BRCA2* expression.

Importantly, *BRCA2* inactivation impairs HR of DSBs and serves as a predictive biomarker for response to treatment with inhibitors of the *PARP1* DNA repair enzyme through synthetic lethality that results from joint inactivation of two DNA repair pathways (HR via *BRCA2* inactivation, and base excision repair via *PARP1* inhibition). Accordingly, treatment of our isogenic cell lines with either a PARP1 inhibitor (olaparib or ABT-888) or radiation resulted in modulation of RAD51 foci formation, which is a component of the HR pathway and a marker for engagement of the HR machinery (18). Specifically, *PCAT-1* overexpression decreased RAD51 foci formation after therapy and *PCAT-1* knockdown increased RAD51 foci formation after therapy in prostate cells (Fig. 1C and Supplementary Fig. S1B–S1D). We further used a well-characterized HR assay, in which cells employ HR to recombine an I-SceI-cut plasmid to produce GFP signaling (16), to evaluate the function of *PCAT-1* on HR directly. We found that transient overexpression of *PCAT-1* in PC3 prostate cancer cells resulted in a significant inhibition of GFP signaling following I-SceI–induced HR in addition to decreased RAD51 foci (Fig. 1D and Supplementary Fig. S2A–S2D). Of note, *PCAT-1* expression does not show substantial change following induction of DNA damage via radiation (Supplementary Fig. S2E).

PCAT-1 expression impairs DNA damage repair

Because *PCAT-1* impairs HR, genotoxic stress of *PCAT-1*–expressing cells should lead to an accumulation of DSBs, which can be visualized using γ-H2AX foci, a marker of DSBs that have not been repaired (4). To test this, we treated our isogenic Du145 and LNCaP cell line models with olaparib, ABT-888, or radiation. As predicted, *PCAT-1* overexpression in Du145 led to an increase in γ-H2AX foci under stress conditions (Fig. 2A and B), indicating that *PCAT-1* impairs DSB repair in these cells. Similarly, LNCaP cells with *PCAT-1* knockdown displayed decreased levels of γ-H2AX foci (Fig. 2A and B). Immunoblot analysis of γ-H2AX protein abundance in these cells following genotoxic stress confirmed a downregulation of γ-H2AX with knockdown of *PCAT-1* and upregulation of γ-H2AX with overexpression of *PCAT-1* (Supplementary Fig. S3).

Finally, we also evaluated the ability for our isogenic cell lines to sustain growth in clonogenic survival assays, a gold-standard assay for cell viability following genotoxic stress, after treatment of cells with PARP1 inhibition or radiation. We found that *PCAT-1* expression led to decreased cell

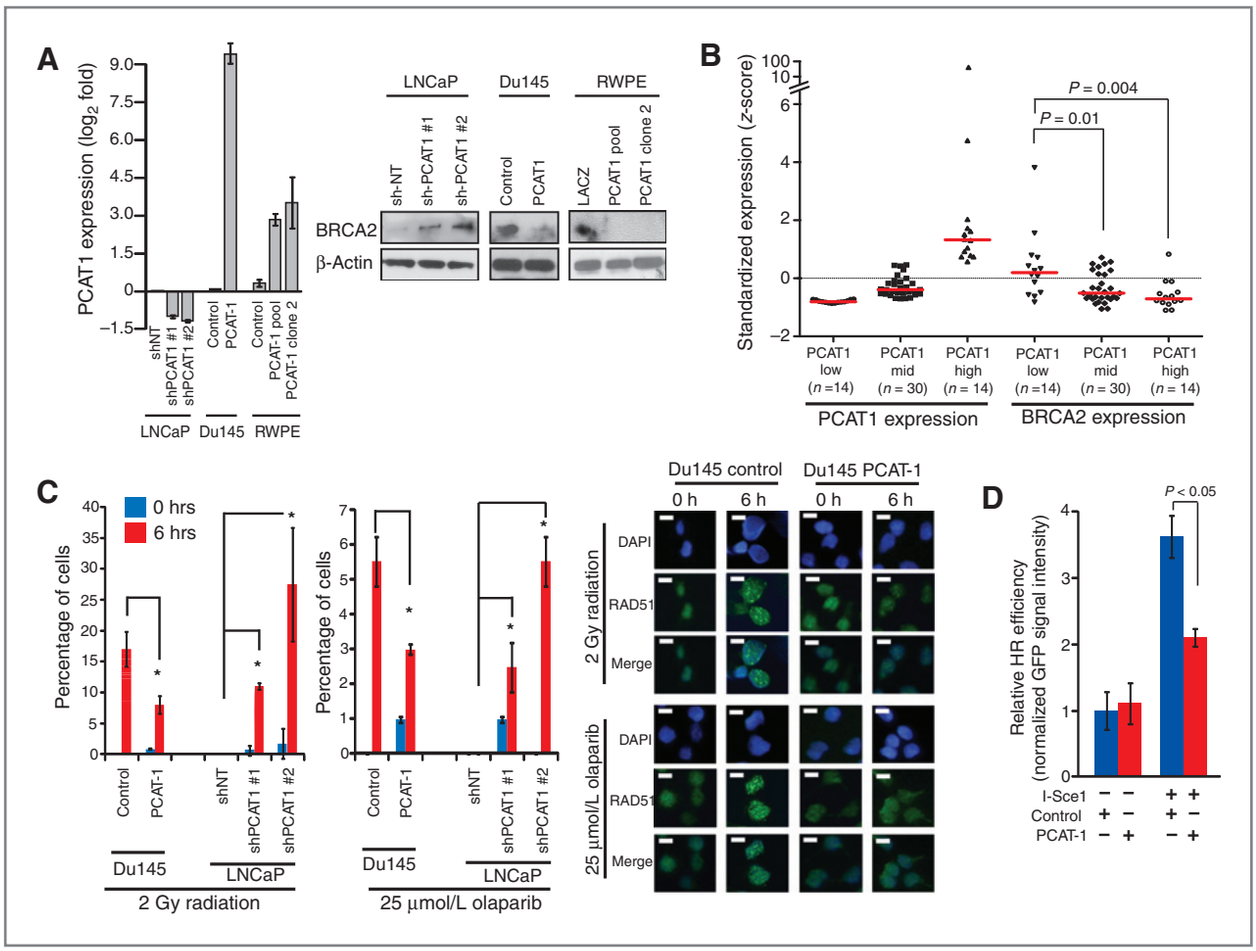

Figure 1. *PCAT-1* expression leads to defective HR in prostate cells. A, left, expression level of *PCAT-1* by quantitative PCR in three isogenic cell lines with overexpression (Du145, RWPE) or knockdown (LNCaP) of *PCAT-1*. Error bars, SEM. Right, Western blot analysis of BRCA2 in three isogenic cell lines with overexpression (Du145, RWPE) or knockdown (LNCaP) of *PCAT-1*. B, expression of *PCAT-1* and *BRCA2* in a cohort of patients with prostate cancer. Expression is shown as *z* scores and stratified by increasing *PCAT-1* expression. *P* values were determined by a Mann–Whitney *U* test. C, left, quantification of RAD51 foci in isogenic Du145 and LNCaP cell lines following 2 Gy of radiation or treatment with 25 μmol/L olaparib. For LNCaP cell line models, cells with >5 foci per cell were quantified. For Du145 cell line models, cells with >10 foci per cell were quantified. Error bars, SD. *, $P < 0.05$ by the Student *t* test. Right, induction of RAD51 foci in Du145-*PCAT-1* cells following 2 Gy of ionizing radiation or treatment with 25 μmol/L olaparib. D, I-SceI–mediated GFP HR assay in PC3-*PCAT-1* cells compared with matched control cells. Error bars, SEM.

survival in Du145 and RWPE cells, whereas *PCAT-1* knockdown increased LNCaP cell survival, in these assays (Supplementary Fig. S4). To exclude a regulatory relationship between *PCAT-1* and other major actors in DNA damage, we performed analysis of XRCC1 (base excision repair pathway), XRCC3 (HR), XRCC4 (NHEJ), Ku70 (NHEJ), Ku80 (NHEJ), and BRCA1 (multiple pathways) in our *in vitro* models, which showed no change in protein abundance upon modulation of *PCAT-1* (Supplementary Fig. S5A). Together, these data indicate that *PCAT-1* expression may impart cell sensitivity to genotoxic stress by decreasing the HR response through downregulation of BRCA2.

PCAT-1 expression leads to increased cell death following genotoxic stress

Because *PCAT-1*–expressing cells exhibit reduced HR efficiency when challenged, we investigated whether PARP1 inhibition selectively killed *PCAT-1*–expressing cells. Following treatment with two PARP1 inhibitors (olaparib or ABT-888), we observed that knockdown of *PCAT-1* in LNCaP cells prevented cell death, whereas overexpression of *PCAT-1* in Du145 and RWPE prostate cells increased cell death in response to PARP inhibition (Fig. 3A, left and Supplementary Fig. S5B–S5D). This change in cell sensitivity to PARP1 inhibitors was striking, with a five-fold change in the IC_{50} for LNCaP and Du145 cells (Fig. 3A, right and Supplementary Fig. S6). Similar results were observed in RWPE cells overexpressing *PCAT-1* (Supplementary Fig. S7).

To ensure that these effects were dependent on BRCA2, we undertook rescue experiments by performing knockdown of *BRCA2* in LNCaP sh*PCAT-1* cells (which have increased levels of BRCA2). These experiments demonstrated a corresponding increase in the sensitivity of these cells to PARP1 inhibition in a

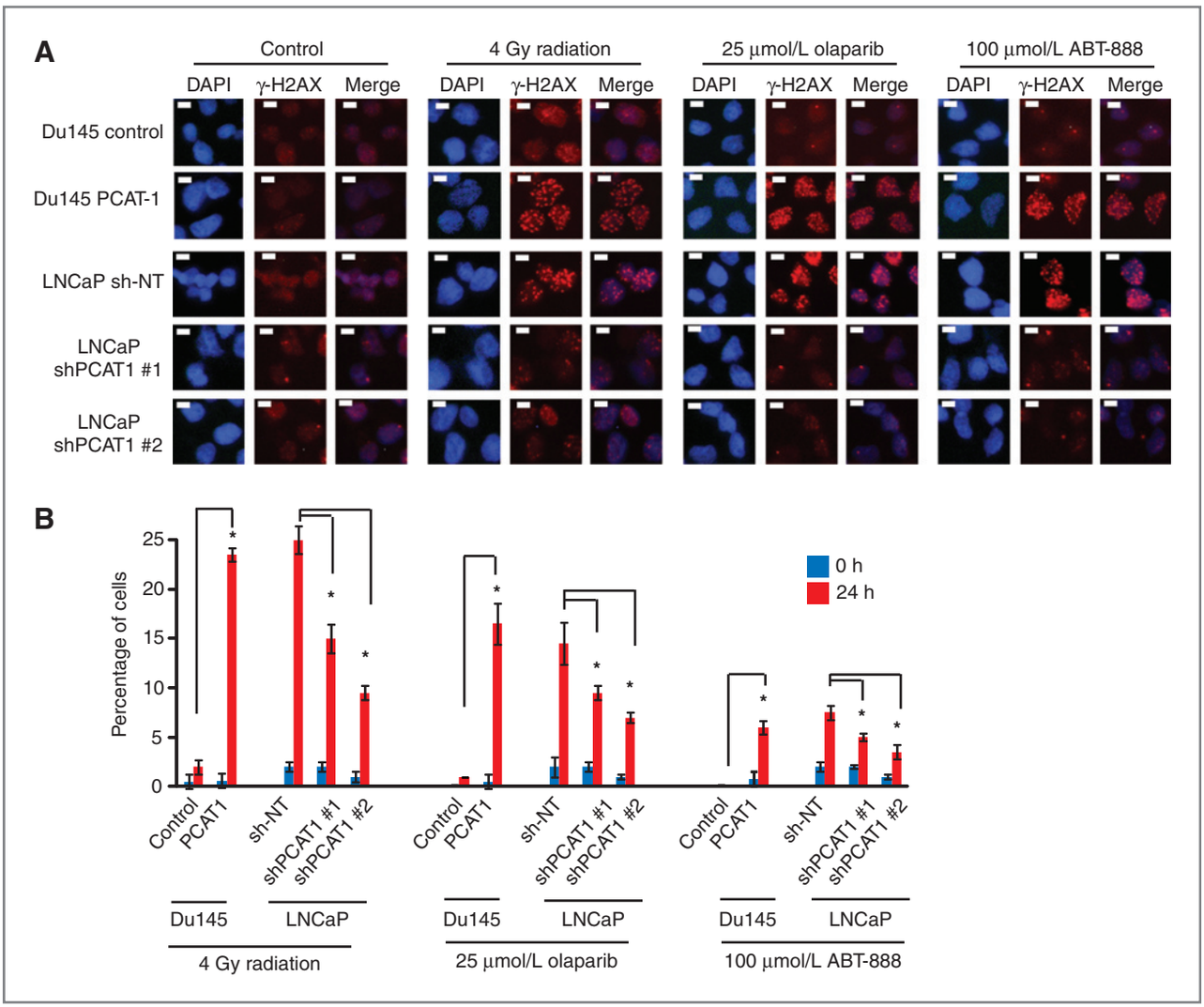

Figure 2. *PCAT-1* knockdown reduces γH2AX foci formation following genotoxic stress. A, LNCaP or Du145 cells with knockdown or overexpression for *PCAT-1* were subjected to 4 Gy of ionizing radiation, 25 μmol/L olaparib, 100 μmol/L of ABT-888, or control DMSO. Twenty-four hours after treatment, cells were fixed and stained for γ-H2AX and counterstained for 4′,6-diamidino-2-phenylindole (DAPI). B, quantification of γ-H2AX foci in LNCaP and Du145 isogenic *PCAT-1* cells treated with radiation or PARP inhibitors. For LNCaP cell line models, cells with >5 foci per cell were quantified. For Du145 cell line models, cells with >10 foci per cell were quantified. Error bars, the SD. *, $P < 0.05$ by the Student *t* test.

dose-dependent manner according to the efficiency of the *BRCA2* knockdown (Fig. 3B). We further observed reduced RAD51 foci after treatment following *BRCA2* knockdown in LNCaP sh*PCAT-1* cells as well (Supplementary Fig. S8). To exclude a role for altered cell-cycle distributions in these phenotypes, we performed flow cytometry, which demonstrated no change in cell cycle in our model systems (Supplementary Fig. S9).

PCAT-1 expression leads to decreased *in vivo* tumor growth following PARP inhibition

To evaluate the contribution of *PCAT-1* to PARP inhibitor response *in vivo*, we generated xenografts of Du145 cells expressing either empty vector control or *PCAT-1*. We observed that Du145-*PCAT-1* cells grew significantly more rapidly in SCID mice, consistent with our previous findings that *PCAT-1* accelerates prostate cell proliferation *in vitro* (Fig. 3C; ref. 10). Moreover, Du145-*PCAT-1* xenografts showed marked susceptibility and tumor regression following intraperitoneal administration of olaparib, whereas Du145-control cells showed only a subtle change in growth while the drug was administered, indicating that the background effect of olaparib therapy, possibly due to its effects on other members of the PARP family (19), is small (Fig. 3C). Mice in all groups of treatment maintained their body weights and showed no evidence of weight loss (Supplementary Fig. S10A).

Importantly, Du145 xenografts retained both *PCAT-1* expression and BRCA2 repression (Fig. 3D). To investigate *PCAT-1* signaling under control-treated (DMSO) and

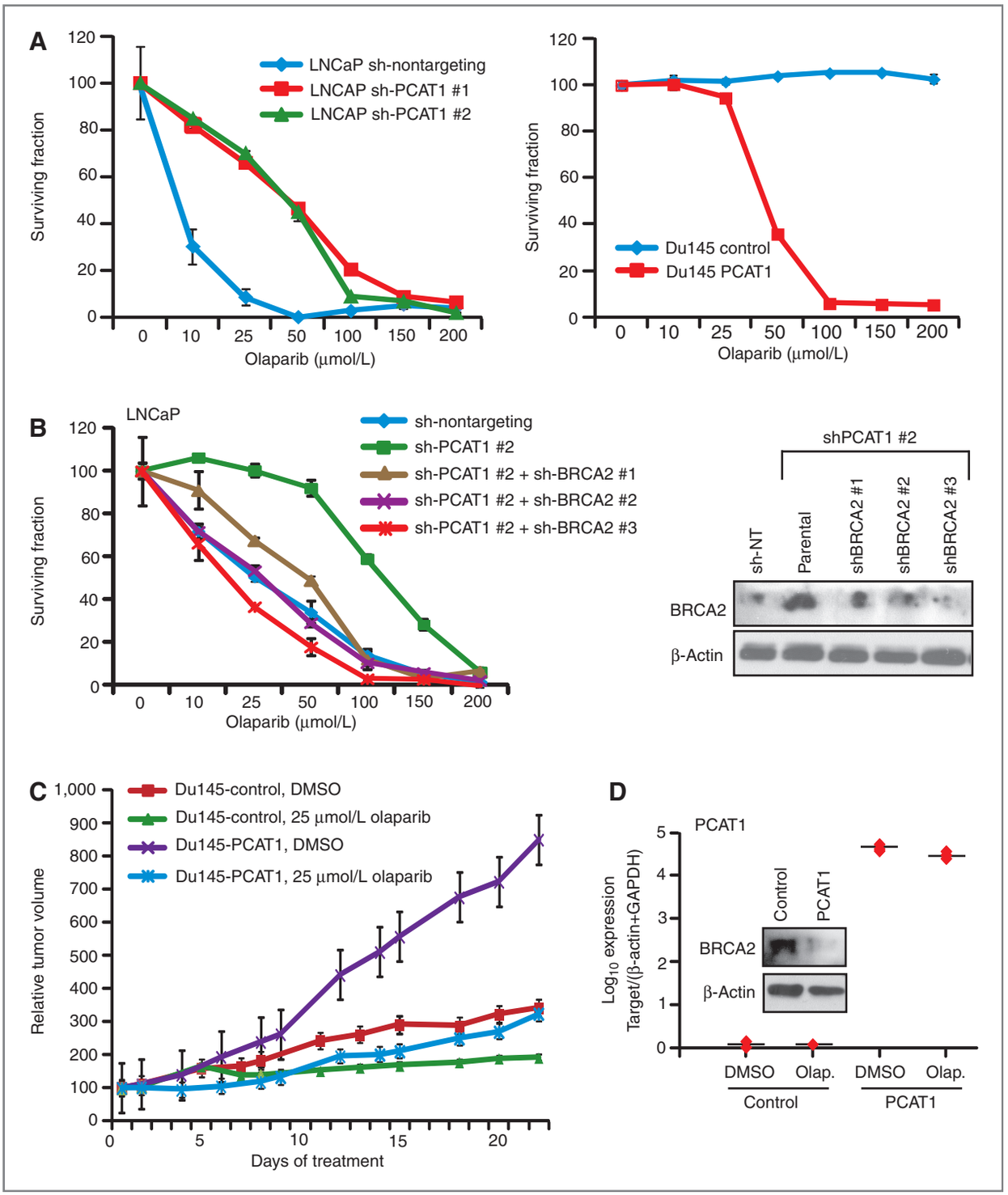

Figure 3. *PCAT-1* expression results in prostate cell sensitivity to PARP inhibition *in vitro* and *in vivo*. A, left, LNCaP cells with *PCAT-1* knockdown exhibit enhanced cell survival 72 hours after treatment with olaparib. Right, Du145 cells with *PCAT-1* overexpression exhibit reduced cell survival 72 hours after treatment with olaparib. Cell survival is determined via WST assays. B, *BRCA2* knockdown in LNCaP sh*PCAT-1* cells rescues cell sensitivity to olaparib. Right, Western blot showing efficiency of BRCA2 knockdown. C, tumor growth curves for Du145-control and Du145-*PCAT-1* xenografts following initiation of treatment with DMSO control or 25 μmol/L olaparib. Tumor volumes are normalized to 100, and time = 0 represents the start of treatment administration. Treatment was initiated 3 weeks after xenograft engraftment. D, expression level of *PCAT-1*and BRCA2 protein in Du145-*PCAT-1* xenografts. Error bars, ± SEM.

olaparib-treated conditions, we also observed *in vivo* upregulation of *PCAT-1*–induced target genes (*TOP2A*, *E2F8*, *BIRC5*, and *KIF15*; Supplementary Fig. S10B) defined by previous microarray profiling of LNCaP cells with *PCAT-1* siRNAs and confirmed in RWPE-*PCAT-1*–overexpressing cells (Supplementary Fig. S10C; ref. 10). These data suggest that *PCAT-1* is mechanistically linked to increased prostate cell sensitivity to PARP1 inhibitors via its repression of BRCA2 both *in vitro* and *in vivo*.

PCAT-1 does not operate via traditional lncRNA-mediated mechanisms

Although many lncRNAs are noted to regulate gene transcription through epigenetic mechanisms (11, 13, 20), we did not observe evidence for this possibility with *PCAT-1*. Although *PCAT-1* regulated *BRCA2* mRNA *in vitro* (Supplementary Fig. S11A), treatment of RWPE-*LacZ* and RWPE-*PCAT-1* cells with the DNA methylation inhibitor 5-azacytidine (5-aza), the histone deacetylase inhibitor TSA, or both, did not reveal enhanced epigenetic regulation of *BRCA2* mRNA in *PCAT-1*–expressing cells (Supplementary Fig. S11B), although there was a baseline regulation of *BRCA2* in both cell lines when 5-aza and TSA were combined. Furthermore, bisulfite sequencing of the *BRCA2* promoter in our isogenic LNCaP and RWPE model systems demonstrated minimal CpG island methylation in all cell lines (Supplementary Fig. S11C). These results suggest that epigenetic repression of *BRCA2* is not the primary mechanism of *PCAT-1*. Moreover, lncRNAs containing Alu elements in their transcript sequence may utilize these repetitive sequences to regulate target gene mRNAs via STAU1-dependent degradation (21). Although *PCAT-1* harbors an Alu element from bps 1103–1402, knockdown of STAU1 in LNCaP or VCaP cells, which endogenously harbor *PCAT-1*, did not alter *BRCA2* levels (Supplementary Fig. S11D).

PCAT-1 regulates BRCA2 post-transcriptionally

To determine whether *PCAT-1* may function in a manner more analogous to microRNAs, which regulate mRNA levels post-transcriptionally (22), we generated a luciferase construct of the *BRCA2* 3′UTR, which is 902 bp in length (Fig. 4A). Surprisingly, we found that RWPE-*PCAT-1* cells, but not control RWPE-*LacZ* cells, were able to directly repress the activity of the wild-type *BRCA2* 3′UTR construct (Fig. 4A). Supporting these data, we found that *PCAT-1* was localized to the cell cytoplasm (Supplementary Fig. S12A) and overexpression of *PCAT-1* in Du145 cells significantly reduced the stability of endogenous *BRCA2* mRNA, consistent with a posttranscriptional mechanism (Supplementary Fig. S12B and S12C).

To map a region of *PCAT-1* required for repression of the *BRCA2* 3′UTR, we additionally generated a series of *PCAT-1* deletion constructs and overexpressed these in RWPE cells (Fig. 4B and Supplementary Fig. S13A). We generated these constructs to establish whether the 3′ end of *PCAT-1*, which contains portions of ancestral transposase and Alu repeat elements (Fig. 4B; ref. 10), or the 5′ end of *PCAT-1*, which consists of nonrepetitive DNA sequences, was required for *BRCA2* repression. We observed that the 5′ end of *PCAT-1* was sufficient to downregulate the *BRCA2* 3′UTR luciferase signal as well as endogenous *BRCA2* transcript levels (Fig. 4B and C), and for this regulation, the first 250 bp of the *PCAT-1* gene were required. In contrast, the 3′ end of *PCAT-1* was expendable. Importantly, the 5′ end of *PCAT-1* was similarly sufficient to sensitize RWPE cells to olaparib treatment *in vitro* (Fig. 4D). To rule out the possibility that RNA instability was responsible for the inactivity of the *PCAT-1* constructs, we performed RNA stability assays, which demonstrated equivalent rates of RNA decay between full-length *PCAT-1* and the inactive *PCAT-1* deletion constructs in RWPE cells (Supplementary Fig. S13B). Together, these results indicate that *PCAT-1* overexpression is able to directly repress the activity of the *BRCA2* 3′UTR and that this repression required the 5′ end of *PCAT-1*.

Discussion

To our knowledge, this is the first report of an lncRNA being involved in the DSB repair process in prostate cancer (Supplementary Fig. S14). These data are supported by a striking inverse correlation between *PCAT-1* and *BRCA2* expression in human prostate cancer samples. Our results expand the potential roles for lncRNAs in cancer biology and contrast strikingly with previous reports that lncRNAs operate epigenetically through chromatin-modifying complexes (23, 24). Indeed, epigenetic regulation likely represents only one of numerous mechanisms for lncRNA function (12, 21, 25, 26). Supporting this notion, we do not observe compelling evidence that *PCAT-1* functions in an epigenetic manner, but rather it may exhibit posttranscriptional regulation of its target genes.

Importantly, *PCAT-1* is also predominantly cytoplasmic, and thus our work describes the first cytoplasmic prostate lncRNA to be associated with therapeutic response. Cytoplasmic lncRNAs are also less well explored than their nuclear counterparts, and our work sheds light onto the complex mechanistic regulation of cellular processes via cytoplasmic lncRNAs. However, *PCAT-1* does exhibit a smaller degree of nuclear expression (see Supplementary Fig. S12A), which may account for our previous observation that *PCAT-1* may associate with the nuclear Polycomb Repressive Complex 2 (PRC2). Although our data directly support a role for *PCAT-1* in the posttranscriptional regulation of *BRCA2*, we cannot fully exclude the possibility of additional regulation of *BRCA2* at the transcriptional level at this time.

In addition, while the mechanism underlying *PCAT-1* function remains incompletely understood, we were intrigued that the 5′ portion of the *PCAT-1* RNA, which is comprised of fully unique sequences, was critical for its regulation of *BRCA2* mRNA whereas the embedded Alu element was not. Although we did not identify a specific microRNA with high-confidence 7-mer complementary base pair matching to both this region of *PCAT-1* and *BRCA2* (data not shown), we speculate that alternative mechanisms of miRNA-like mismatch base pairing

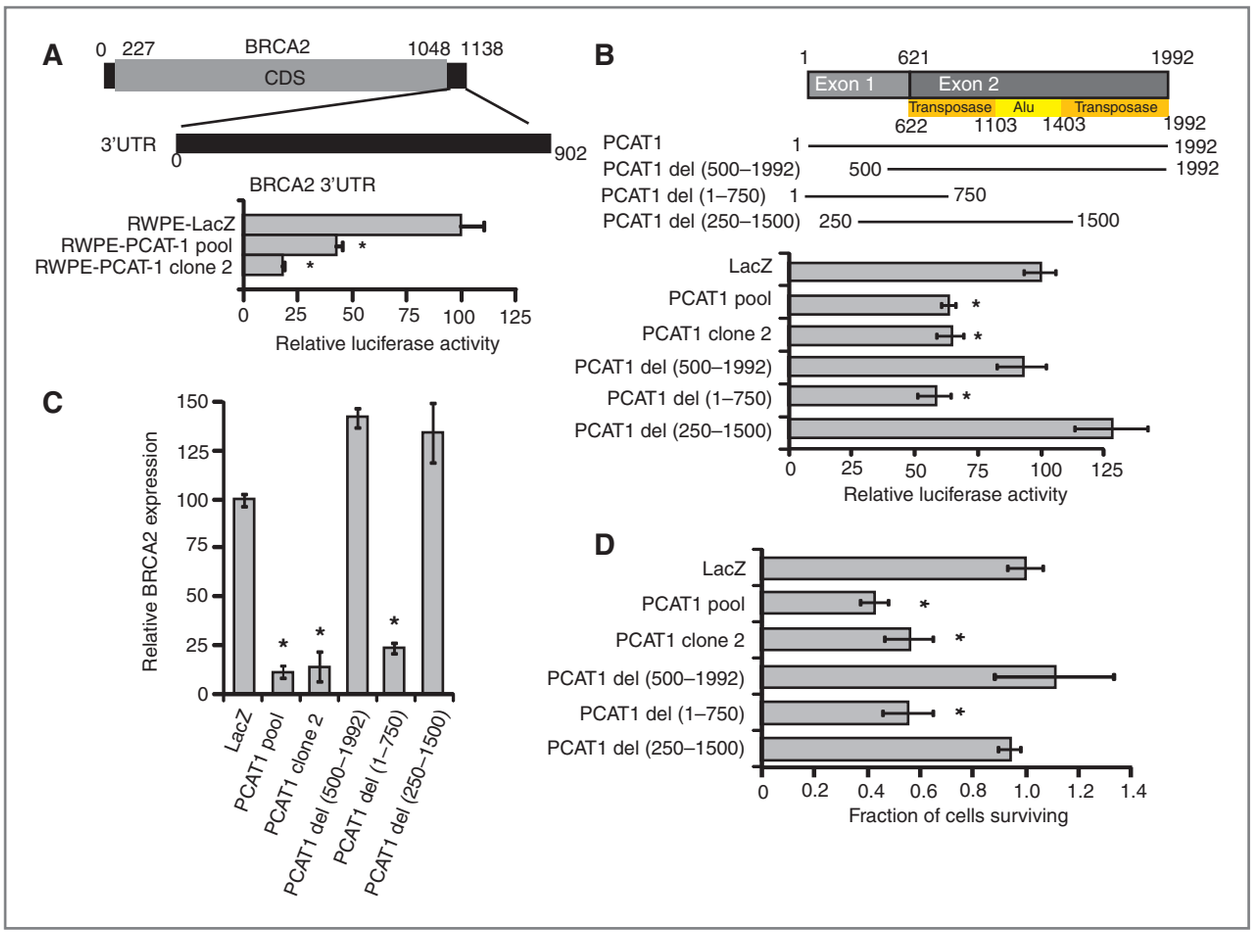

Figure 4. The 5′ terminus of *PCAT-1* represses *BRCA2* mRNA via the 3′UTR of *BRCA2*. A, transfection of a *BRCA2* 3′UTR luciferase construct in RWPE-*PCAT-1* cells. B, a schematic of *PCAT-1* deletion constructs overexpressed in RWPE cells. *PCAT-1* del (1-750 bps) was able to recapitulate repression of the *BRCA2* 3′UTR luciferase construct. C, endogenous *BRCA2* transcript levels in RWPE cells overexpressing *PCAT-1* deletion constructs. D, treatment of RWPE cells overexpressing *PCAT-1* deletion constructs with 25 μmol/L olaparib. Cell survival was measured 72 hours after treatment with WST. Error bars, ± SEM. *, $P < 0.05$ by the Student *t* test.

may contribute to *PCAT-1*-mediated regulation in a manner similar to the recently described networks of competing endogenous RNAs (27).

Together, our data suggest that lncRNAs may have a more widespread role in mammalian genome maintenance and DNA repair than previously appreciated. In support of this, a role for small RNAs in human DNA damage repair in human cells has been recently reported and shown to be dependent upon the microRNA biogenesis machinery (28). Of note, Adamson and colleagues nominated the RNA-binding protein *RBMX* as a novel component of the HR pathway (16), suggesting that RNA–protein interactions may be integral to this process.

This work sheds insight onto potential mechanisms of impaired DSB repair in cancers lacking an inactivating mutation in canonical DSB repair proteins. Thus, our studies have uncovered a novel mechanism of "BRCAness"—the clinical observation that many cancers lacking BRCA1/BRCA2 mutations exhibit the clinical features of impaired DSB repair (2, 29, 30). We hypothesize that other cancers with a BRCA-like phenotype may harbor lncRNAs involved in the regulation and execution of proper HR and other forms of DSB repair. Finally, future clinical trials examining the efficacy of PARP1 inhibitors in prostate cancer will provide critical information as to whether *PCAT-1* may serve as a predictive biomarker for patient response to PARP1 inhibitor therapy.

Disclosure of Potential Conflicts of Interest

J.R. Prensner has ownership interest (including patents) in patent on PCAT1 and ncRNAs in prostate cancer. A.K. Tewari has honoraria from speakers' bureau from Intuitive Surgical, has ownership interest (including patents) in the US Patents US 6004267 A—Method for diagnosing and staging prostate cancer and US 8241310 B2—Urethral catheterless radical prostatectomy. A.M. Chinnaiyan has ownership interest (including patents) in Gen-Probe and Wafergen and is a consultant/advisory board member of Wafergen. No potential conflicts of interests were disclosed by the other authors.

Authors' Contributions

Conception and design: J.R. Prensner, W. Chen, C.J. Logothetis, A.K. Tewari, A. M. Chinnaiyan, F.Y. Feng

Development of methodology: J.R. Prensner, W. Chen, T. Ma, A.K. Tewari F.Y. Feng
Acquisition of data (provided animals, acquired and managed patients, provided facilities, etc.): J.R. Prensner, W. Chen, Q. Cao, T. Ma, S. Han, A. Sahu, R. Malik, K. Wilder-Romans, N. Navone, L.L. Pisters, A.K. Tewari, N. Kitabayashi, M.A. Rubin, F. Demichelis, F.Y. Feng
Analysis and interpretation of data (e.g., statistical analysis, biostatistics, computational analysis): J.R. Prensner, W. Chen, M.K. Iyer, T. Ma, L.L. Pisters, A.K. Tewari, K.E. Knudsen, F. Demichelis, T.S. Lawrence, F.Y. Feng
Writing, review, and/or revision of the manuscript: J.R. Prensner, W. Chen, N. Navone, C.J. Logothetis, L.L. Pisters, A.K. Tewari, T.S. Lawrence, A.M. Chinnaiyan, F.Y. Feng
Administrative, technical, or material support (i.e., reporting or organizing data, constructing databases): C.J. Logothetis, J.C. Araujo, A.K. Tewari, F.Y. Feng
Study supervision: A.M. Chinnaiyan, F.Y. Feng
Provided experimental design input regarding analyzing homologous recombination in cells: C.E. Canman

Acknowledgments

The authors thank Mats Ljungman, Saravana M. Dhanasekaran, Chad Brenner, Yi-Mi Wu, Daniel Robinson, Sameek Roychowdhury, and Dan Hamstra for helpful discussions. The authors also thank Benjamin Chandler for technical assistance.

Grant Support

This work was supported in part by the Prostate Cancer Foundation (F.Y. Feng and A.M. Chinnaiyan), NIH Prostate Specialized Program of Research Excellence grant P50CA69568, Department of Defense grants PC094231 (F.Y. Feng) and PC100171 (A.M. Chinnaiyan), the Early Detection Research Network grant UO1 CA111275 (A.M. Chinnaiyan), the Prostate Cancer Foundation-Movember Challenge Award (K.E. Knudsen, F.Y. Feng, and M.A. Rubin), the U.S. National Institutes of Health R01CA132874-01A1 (A.M. Chinnaiyan) and R01CA152057 (M.A. Rubin and F. Demichelis), and the National Center for Functional Genomics support by the Department of Defense (A.M. Chinnaiyan). A.M. Chinnaiyan is also supported by the Doris Duke Charitable Foundation Clinical Scientist Award and the Howard Hughes Medical Institute. A.M. Chinnaiyan is an American Cancer Society Research Professor and a Taubman Scholar of the University of Michigan. J.R. Prensner, M.K. Iyer, and Q. Cao were supported by the Department of Defense Fellowship grants PC094290 (J.R. Prensner), BC100238 (M.K. Iyer), and PC094725 (Q. Cao). J.R. Prensner was supported by a Prostate Cancer Foundation Young Investigator award. J.R. Prensner, A. Sahu, and M.K. Iyer are Fellows of the University of Michigan Medical Scientist Training Program.

The costs of publication of this article were defrayed in part by the payment of page charges. This article must therefore be hereby marked *advertisement* in accordance with 18 U.S.C. Section 1734 solely to indicate this fact.

Received November 4, 2013; revised January 7, 2014; accepted January 9, 2014; published OnlineFirst January 28, 2014.

References

1. Negrini S, Gorgoulis VG, Halazonetis TD. Genomic instability–an evolving hallmark of cancer. Nat Rev Mol Cell Biol 2010;11:220–8.
2. Turner N, Tutt A, Ashworth A. Hallmarks of 'BRCAness' in sporadic cancers. Nat Rev Cancer 2004;4:814–9.
3. Turner NC, Reis-Filho JS, Russell AM, Springall RJ, Ryder K, Steele D, et al. BRCA1 dysfunction in sporadic basal-like breast cancer. Oncogene 2007;26:2126–32.
4. Jackson SP, Bartek J. The DNA-damage response in human biology and disease. Nature 2009;461:1071–8.
5. Roy R, Chun J, Powell SN. BRCA1 and BRCA2: different roles in a common pathway of genome protection. Nat Rev Cancer 2012;12:68–78.
6. Farmer H, McCabe N, Lord CJ, Tutt AN, Johnson DA, Richardson TB, et al. Targeting the DNA repair defect in BRCA mutant cells as a therapeutic strategy. Nature 2005;434:917–21.
7. Bryant HE, Schultz N, Thomas HD, Parker KM, Flower D, Lopez E, et al. Specific killing of BRCA2-deficient tumours with inhibitors of poly(ADP-ribose) polymerase. Nature 2005;434:913–7.
8. Fong PC, Boss DS, Yap TA, Tutt A, Wu P, Mergui-Roelvink M, et al. Inhibition of poly(ADP-ribose) polymerase in tumors from BRCA mutation carriers. N Engl J Med 2009;361:123–34.
9. Huarte M, Rinn JL. Large non-coding RNAs: missing links in cancer? Hum Mol Genet 2010;19:R152–61.
10. Prensner JR, Iyer MK, Balbin OA, Dhanasekaran SM, Cao Q, Brenner JC, et al. Transcriptome sequencing across a prostate cancer cohort identifies PCAT-1, an unannotated lincRNA implicated in disease progression. Nat Biotechnol 2011;29:742–9.
11. Gupta RA, Shah N, Wang KC, Kim J, Horlings HM, Wong DJ, et al. Long non-coding RNA HOTAIR reprograms chromatin state to promote cancer metastasis. Nature 2010;464:1071–6.
12. Prensner JR, Chinnaiyan AM. The emergence of lncRNAs in cancer biology. Cancer Discov 2011;1:391–407.
13. Rinn JL, Kertesz M, Wang JK, Squazzo SL, Xu X, Brugmann SA, et al. Functional demarcation of active and silent chromatin domains in human HOX loci by noncoding RNAs. Cell 2007;129:1311–23.
14. Wan G, Hu X, Liu Y, Han C, Sood AK, Calin GA, et al. A novel non-coding RNA lncRNA-JADE connects DNA damage signalling to histone H4 acetylation. EMBO J 2013;32:2833–47.
15. Wan G, Mathur R, Hu X, Liu Y, Zhang X, Peng G, et al. Long non-coding RNA ANRIL (CDKN2B-AS) is induced by the ATM-E2F1 signaling pathway. Cell Signal 2013;25:1086–95.
16. Adamson B, Smogorzewska A, Sigoillot FD, King RW, Elledge SJ. A genome-wide homologous recombination screen identifies the RNA-binding protein RBMX as a component of the DNA-damage response. Nat Cell Biol 2012;14:318–28.
17. Weinstock DM, Nakanishi K, Helgadottir HR, Jasin M. Assaying double-strand break repair pathway choice in mammalian cells using a targeted endonuclease or the RAG recombinase. Methods Enzymol 2006;409:524–40.
18. Baumann P, Benson FE, West SC. Human Rad51 protein promotes ATP-dependent homologous pairing and strand transfer reactions *in vitro*. Cell 1996;87:757–66.
19. Wahlberg E, Karlberg T, Kouznetsova E, Markova N, Macchiarulo A, Thorsell AG, et al. Family-wide chemical profiling and structural analysis of PARP and tankyrase inhibitors. Nat Biotechnol 2012;30:283–8.
20. Wang KC, Yang YW, Liu B, Sanyal A, Corces-Zimmerman R, Chen Y, et al. A long noncoding RNA maintains active chromatin to coordinate homeotic gene expression. Nature 2011;472:120–4.
21. Gong C, Maquat LE. lncRNAs transactivate STAU1-mediated mRNA decay by duplexing with 3′ UTRs via Alu elements. Nature 2011;470:284–8.
22. Bartel DP. MicroRNAs: target recognition and regulatory functions. Cell 2009;136:215–33.
23. Tsai MC, Manor O, Wan Y, Mosammaparast N, Wang JK, Lan F, et al. Long noncoding RNA as modular scaffold of histone modification complexes. Science 2010;329:689–93.
24. Prensner JR, Iyer MK, Sahu A, Asangani IA, Cao Q, Patel L, et al. The long noncoding RNA SChLAP1 promotes aggressive prostate cancer and antagonizes the SWI/SNF complex. Nat Genet 2013;45:1392–8.
25. Wang D, Garcia-Bassets I, Benner C, Li W, Su X, Zhou Y, et al. Reprogramming transcription by distinct classes of enhancers functionally defined by eRNA. Nature 2011;474:390–4.
26. Cesana M, Cacchiarelli D, Legnini I, Santini T, Sthandier O, Chinappi M, et al. A long noncoding RNA controls muscle differentiation by functioning as a competing endogenous RNA. Cell 2011;147:358–69.

27. Salmena L, Poliseno L, Tay Y, Kats L, Pandolfi PP. A ceRNA hypothesis: the Rosetta Stone of a hidden RNA language? Cell 2011;146:353–8.
28. Francia S, Michelini F, Saxena A, Tang D, de Hoon M, Anelli V, et al. Site-specific DICER and DROSHA RNA products control the DNA-damage response. Nature 2012;488:231–5.
29. Konstantinopoulos PA, Spentzos D, Karlan BY, Taniguchi T, Fountzilas E, Francoeur N, et al. Gene expression profile of BRCAness that correlates with responsiveness to chemotherapy and with outcome in patients with epithelial ovarian cancer. J Clin Oncol 2010;28:3555–61.
30. Oonk AM, van Rijn C, Smits MM, Mulder L, Laddach N, Savola SP, et al. Clinical correlates of 'BRCAness' in triple-negative breast cancer of patients receiving adjuvant chemotherapy. Ann Oncol 2012;23:2301–5.